Asymmetric Pentacene Derivatives for Organic Light-Emitting Diodes

Bo-Bin Jang,† Sang Ho Lee,† and Zakya H. Kafafi*

Optical Sciences Division, U.S. Naval Research Laboratory, Washington, D.C. 20375

Received September 14, 2005. Revised Manuscript Received November 1, 2005

Two aryl-substituted red emitting pentacenes, 5,6,13,14-tetraphenylpentacene (*asym*-TPP) and 5,14-bis(2,6-dimethylphenyl)-6,13-diphenylpentacene (DMPDPP), have been prepared and spectroscopically characterized. Guest−host films of pentacene derivatives dispersed in tris(quinolin-8-olato)aluminum(III) (Alq_3) exhibit narrow red emission ($\lambda_{max} = 663-680$ nm), indicative of efficient Förster energy transfer from the Alq_3 host to the guest molecules. Solid-state absolute photoluminescence quantum yields of the films were measured as a function of guest molecule concentration ($\Phi_{PL} \sim 20\%$ at 0.20−0.50 mol %). Red light-emitting diodes based on the fluorescent DMPDPP yield external electroluminescence quantum efficiency ($\eta_{EL} \sim 1\%$) close to the theoretical limit.

Introduction

Polycyclic aromatic hydrocarbons (PAHs), especially linear PAHs, have played a major role as electroactive materials due to their attractive molecular and electronic structure.[1] They exhibit good intermolecular $\pi-\pi$ overlap in the solid state, normally face-to-edge (herringbone) packing,[2] due to their extended π-conjugation and rigid planarity, which gives rise to high charge carrier mobilities in the solid state. Pentacene derivatives, linear PAHs consisting of five laterally fused benzene rings, have been used as the electronic material of choice in p-type organic field-effect transistors (OFETs).[3−8] Recently, high hole mobilities ($\mu > 1$ cm^2/V s) have been reported for OFETs based on pentacene.[4b,5,6a] This was attributed to the remarkably low reorganization energy, which is caused by the small structural change upon going from the neutral-state geometry to the charged-state geometry and vice versa.[9] In an attempt to improve solubility and effective solid-state molecular ordering, Anthony et al. prepared a number of pentacene derivatives, in which the functional group induces self-assembly of the aromatic moieties into highly ordered π-stacked arrays (i.e., enhanced intermolecular orbital overlap) leading to high carrier mobilities.[6]

Pentacene and its derivatives have also been used as the light-harvesting materials in organic photovoltaic cells (OPVs)[10,11] and as the emitters in organic light-emitting diodes (OLEDs).[12−14] In particular, diaryl-substituted derivatives of pentacene have been used as red emitters in OLEDs.[12−14] Fine-tuning of their emissive properties was achieved by effectively controlling the π-conjugation length through facile substitution at multiple positions while maintaining their relatively high photoluminescence (PL) quantum yields.[15,16] Although many red emitters based on the pyran skeleton have been designed, they exhibit poor color chromaticity (orange-red) due to their broad emission spectra. More recently, triplet emitters (i.e., phosphorescent materials) based on rare-earth metal complexes such as europium(III) chelates[17−21] and iridium(III)[22−26] and ruthe-

* To whom correspondence should be addressed. E-mail: kafafi@nrl.navy.mil.

† Also at SFA Inc., Largo, MD 20774.

(1) (a) Watson, M. D.; Fechtenkötter, A.; Müllen, K. *Chem. Rev.* **2001**, *101*, 1267. (b) Brédas, J.-L.; Beljonne, D.; Coropceanu, V.; Cornil, J. *Chem. Rev.* **2004**, *104*, 4971. (c) Kelley, T. W.; Baude, P. F.; Gerlach, C.; Ender, D. E.; Muyres, D.; Haase, M. A.; Vogel, D. E.; Theiss, S. D. *Chem. Mater.* **2004**, *16*, 4413.

(2) Desiraju, G. R.; Gavezzotti, A. *Acta Crystallogr., Sect. B* **1989**, *45*, 473.

(3) For reviews: (a) Katz, H. E.; Bao, Z.; Gilat, S. L. *Acc. Chem. Res.* **2001**, *34*, 359. (b) Dimitrakopoulos, C. D.; Malenfant, P. R. L. *Adv. Mater.* **2002**, *14*, 99.

(4) (a) Nelson, S. F.; Lin, Y.-Y.; Gundlach, D. J.; Jackson, T. N. *Appl. Phys. Lett.* **1998**, *72*, 1854. (b) Sheraw, C. D.; Zhou, L.; Huang, J. R.; Gundlach, D. J.; Jackson, T. N.; Kane, M. G.; Hill, I. G.; Hammond, M. S.; Campi, J.; Greening, B. K.; Francl, J.; West, J. *Appl. Phys. Lett.* **2002**, *80*, 1088.

(5) Klauk, H.; Halik, M.; Zschieschang, U.; Schmid, G.; Radlik, W.; Weber, W. *J. Appl. Phys.* **2002**, *92*, 5259.

(6) (a) Anthony, J. E.; Brooks, J. S.; Eaton, D. L.; Parkin, S. R. *J. Am. Chem. Soc.* **2001**, *123*, 9482. (b) Payne, M. M.; Parkin, S. R.; Anthony, J. E.; Kuo, C.-C.; Jackson, T. N. *J. Am. Chem. Soc.* **2005**, *127*, 4986.

(7) Afzali, A.; Dimitrakopoulos, C. D.; Breen, T. L. *J. Am. Chem. Soc.* **2002**, *124*, 8812.

(8) Sakamoto, Y.; Suzuki, T.; Kobayashi, M.; Gao, Y.; Fukai, Y.; Inoue, Y.; Sato, F.; Tokito, S. *J. Am. Chem. Soc.* **2004**, *126*, 8138.

(9) Gruhn, N. E.; da Silva Filho, D. A.; Bill, T. G.; Malagoli, M.; Coropceanu, V.; Kahn, A.; Brédas, J. L. *J. Am. Chem. Soc.* **2002**, *124*, 7918.

(10) Senadeera, G. K. R.; Jayaweera, P. V. V.; Perera, V. P. S.; Tennakone, K. *Sol. Energy Mater. Sol. Cells* **2002**, *73*, 103.

(11) Mayer, A. C.; Lloyd, M. T.; Hermann, D. J.; Kasen, T. G.; Malliaras, G. G. *Appl. Phys. Lett.* **2004**, *85*, 6272.

(12) Picciolo, L. C.; Murata, H.; Kafafi, Z. H. *Appl. Phys. Lett.* **2001**, *78*, 2378.

(13) Picciolo, L. C.; Murata, H.; Gondarenko, A.; Noda, T.; Shirota, Y.; Eaton, D. L.; Anthony, J. E.; Kafafi, Z. H. *Proc. SPIE-Int. Soc. Opt. Eng.* **2002**, *4464*, 383.

(14) Wolak, M. A.; Jang, B.-B.; Palilis, L. C.; Kafafi, Z. H. *J. Phys. Chem. B* **2004**, *108*, 5492.

(15) (a) Payne, M. M.; Delcamp, J. H.; Parkin, S. R.; Anthony, J. E. *Org. Lett.* **2004**, *6*, 1609. (b) Payne, M. M.; Odom, S. A.; Parkin, S. R.; Anthony, J. E. *Org. Lett.* **2004**, *6*, 3325.

(16) Duong, H. M.; Bendikov, M.; Steiger, D.; Zhang, Q.; Sonmez, G.; Yamada, J.; Wudl, F. *Org. Lett.* **2003**, *5*, 4433.

(17) Kido. J.; Nagai, K.; Okamoto, Y.; Skotheim, T. *Chem. Lett.* **1991**, 1267.

(18) Adachi, C.; Baldo, M. A.; Forrest, S. R. *J. Appl. Phys.* **2000**, *87*, 8049.

10.1021/cm052069h CCC: $33.50
Published on Web 12/30/2005

nium(III) complexes,[27] have been used to improve the performance of the red-emitting OLED. For example, a red-emitting device based on an iridium complex, Ir(1-phenylisoquinolinato)$_3$, shows a very high external electroluminescence (EL) quantum efficiency ($\eta_{EL} = 10.3\%$).[26] One of the main problems of OLEDs based on phosphorescent dyes is that they typically display rapid decline in EL quantum efficiency at high current density due to triplet−triplet annihilation.[22,28−29] This is not the case for the OLEDs based on the fluorescent dyes (i.e., pentacene derivatives) which exhibit stable EL quantum efficiency that is not dependent on current densities.[12,14,30]

Recently, we developed OLEDs based on pentacene derivatives substituted with alkynyl (ethynyl-*tert*-butyl and ethynyl-silane) or aryl (phenyl, 2,6-dimethylphenyl, and 4-*tert*-butylphenyl) moieties at the 6,13 position of the pentacene skeleton.[12−14] The emission maxima ($\lambda_{max} = 670$ nm) of the pentacene derivatives with alkynyl moieties (DAP derivatives) dispersed in tris(quinolin-8-olato)aluminum(III) (Alq_3) showed large red-shifts with respect to those incorporating the aryl moieties (DPP derivatives). DPP derivatives exhibited saturated red emission (615−630 nm) with reasonably high PL quantum yields ($\Phi_{PL} \sim 30\%$) when dispersed in Alq_3. In particular, red-emitting devices based on pentacene derivatives exhibited external EL quantum efficiencies ($\eta_{EL} = 1.3-1.4\%$) close to the estimated theoretical limit (1.5%).[12,14]

Here, we report on the synthesis and spectroscopic characterization of pentacene derivatives incorporating elements of the rubrene ($\Phi_{PL} = 100\%$) molecular structure, in an effort to increase their PL quantum yields while maintaining their saturated red emission. We first give details with regard to the synthesis of 5,6,13,14-tetraphenylpentacene (*asym*-TPP) and 5,14-bis(2,6-dimethylphenyl)-6,13-diphenylpentacene (DMPDPP), featuring four aryl substituents asymmetrically affixed to the pentacene core. Then, we discuss the photo-oxidative and electrochemical stability of these asymmetrically functionalized pentacene derivatives in solution followed by their electronic and optical properties in solution and in the solid-state. Finally, we incorporate them as active emissive layers in OLED structures and evaluate their performance.

(19) Zhu, W.; Jiang, Q.; Lu, Z.; Wei, X.; Xie, M.; Zou, D.; Tsutsui, T. *Thin Solid Films* **2000**, *363*, 167.
(20) Sun, P.-P.; Duan, J.-P.; Shih, H.-T.; Cheng, C.-H. *Appl. Phys. Lett.* **2002**, *81*, 792.
(21) Liang, F.; Zhou, Q.; Cheng, Y.; Wang, L.; Ma, D.; Jing, X.; Wang, F. *Chem. Mater.* **2003**, *15*, 1935.
(22) Adachi, C.; Baldo, M. A.; Forrest, S. R.; Lamansky, S.; Thompson, M. E.; Kwong, R. C. *Appl. Phys. Lett.* **2001**, *78*, 1622.
(23) Kawamura, Y.; Yanagida, S.; Forrest, S. R. *J. Appl. Phys.* **2002**, *92*, 87.
(24) Gong, X.; Ostrowski, J. C.; Bazan, G. C.; Moses, D.; Heeger, A. J. *Appl. Phys. Lett.* **2002**, *81*, 3711.
(25) Duan, J.-P.; Sun, P.-P.; Cheng, C.-H. *Adv. Mater.* **2003**, *15*, 224.
(26) Tsuboyama, A.; Iwawaki, H.; Furugori, M.; Mukaide, T.; Kamatani, J.; Igawa, S.; Moriyama, T.; Miura, S.; Takiguchi, T.; Okada, S.; Hoshino, M.; Ueno, K. *J. Am. Chem. Soc.* **2003**, *125*, 12971.
(27) Gao, F. G.; Bard, A. J. *J. Am. Chem. Soc.* **2000**, *122*, 7426.
(28) Baldo, M. A.; O'Brien, D. F.; Thompson, M. E.; Forrest, S. R. *Phys. Rev. B* **1999**, *60*, 14422.
(29) Baldo, M. A.; Adachi, C.; Forrest, S. R. *Phys. Rev. B* **2000**, *62*, 10967.
(30) Mi, B. X.; Gao, Z. Q.; Liu, M. W.; Chan, K. Y.; Kwong, H. L.; Wong, N. B.; Lee, C. S.; Hung, L. S.; Lee, S. T. *J. Mater. Chem.* **2002**, *12*, 1307.

Experimental Section

General. All commercially available chemicals, reagents, and solvents were used as received without further purification unless otherwise stated. Tetrahydrofuran was distilled over sodium/benzophenone under dry nitrogen, and CH_2Cl_2 was predried by standing overnight in hot molecular sieves (4 Å). ^{1}H and ^{13}C NMR spectra were recorded on a Bruker 300 MHz NMR spectrometer using tetramethylsilane (TMS, 0.00 ppm) as the internal reference. Column chromatography was performed with 32−63 mesh silica gel. Cyclic voltammetry was performed on a Bioanalytical Systems Inc. model CV-50W potentiostat in a three-electrode cell with a Pt counter electrode, a $Ag/AgNO_3$ reference electrode, and a glassy carbon working electrode at a scan rate of 100 mV/s with 0.1 M tetrabutylammonium perchlorate as the supporting electrolyte in degassed 1,2-dichlorobenzene solution purged with argon. At the end of each set of voltammetric experiments, ferrocene (Fc) was added to the solution in order to correct the observed potential with a Fc/Fc^+ reference potential. Elemental analyses were performed by Quantitative Technologies Inc. (QTI). Mass spectrometry was carried out on M-Scan's VG analytical ZAB 2-SE high field mass spectrometer. All organic materials were purified prior to use via duplicate train sublimation ($\sim 5.0 \times 10^{-6}$ Torr). 5,7,12,14-Tetraphenylpentacene (*sym*-TPP)[31] and 6,13-diphenylpentacene-5,14-quinone (**1**)[32] were synthesized as previously reported.

5,6,13,14-Tetraphenylpentacene-5,14-diol (2). To a round-bottom flask containing pentacenequinone **1** (0.91 g, 1.97 mmol) was added THF (200 mL) under nitrogen atmosphere. The mixture was cooled to 0 °C and stirred for 15 min. Phenylmagnesium bromide (19.7 mL of a 1.0 M solution in THF, 19.7 mmol) was transferred slowly by cannula to the solution of pentacenequinone **1**. The resulting dark mixture was warmed to room temperature and stirred for 1 h. The reaction mixture was refluxed for 5 h, followed by quenching with aqueous NH_4Cl. The organic residue was subsequently extracted with ethyl acetate, washed with brine, dried over $MgSO_4$, and concentrated in vacuo to give crude red solid. The crude product was purified by column chromatography (silica gel, hexane/chloroform = 1/1) and subsequent recrystallization from ethyl acetate/hexane to afford pure diol **2** (0.36 g, yield 30%). ^{1}H NMR (CD_2Cl_2): δ 7.55−7.59 (dd, $J = 6.5$, 3.3 Hz, 2H), 7.51 (s, 2H), 7.25−7.38 (m, 8H), 6.90−7.16 (m, 16H), 6.27 (d, $J = 7.7$ Hz, 2H), 3.71 (s, 2H). ^{13}C NMR (CD_2Cl_2): δ 150.4, 141.1, 140.1, 138.3, 136.9, 133.4, 132.0, 131.9, 131.6, 129.2, 128.5, 127.9, 127.7, 127.5, 126.7, 126.3, 126.1, 126.0, 75.8.

5,6,13,14-Tetraphenylpentacene (*asym*-TPP) (3). To a solution of diol **2** (0.20 g, 0.32 mmol) in THF (50 mL) was added 3 mL of aqueous HI (55−57%). Care was taken to ensure the solution was not exposed to ambient light. The dark mixture was allowed to react for 10 s, at which point a solid was deposited in the reaction mixture. After immediate filtering, the solid was washed with saturated aqueous $Na_2S_2O_5$ (3 × 100 mL), water (3 × 100 mL), and cold MeOH (3 × 100 mL), respectively. The solid was dissolved in diethyl ether, and the organic layer was washed with aqueous KOH (1 M) and subsequently with saturated brine. The organic layer was dried over $MgSO_4$ and concentrated in vacuo at room temperature. Double recrystallization from diethyl ether/hexane afforded pure product **3** as blue solid (50 mg, yield 27%). ^{1}H NMR ($CDCl_3$): δ 8.01 (s, 2H), 7.55−7.59 (dd, $J = 6.6$, 3.1 Hz, 2H), 7.25−7.30 (m, 4H), 6.97−7.21 (m, 18H), 6.85−6.87 (d, $J = 6.8$ Hz, 4H). ^{13}C NMR ($CDCl_3$): δ 142.0, 141.9, 136.8, 136.6, 132.6, 132.0, 131.2, 130.1, 129.5, 128.8, 128.5, 127.3, 127.2, 126.7,

(31) (a) Allen, C. F. H.; Bell, A. *J. Am. Chem. Soc.* **1942**, *64*, 1253. (b) Sparfel, D.; Gobert, F.; Rigaudy, J. *Tetrahedron* **1980**, *36*, 2225.
(32) Cava, M. P.; VanMeter, J. P. *J. Org. Chem.* **1969**, *34*, 538.

125.9, 125.7, 125.1, 124.9, 124.8. Anal. Calcd for $C_{46}H_{30}$: C, 94.81; H, 5.19. Found: C, 94.75; H, 5.17.

5,14-Bis(2,6-dimethylphenyl)-6,13-diphenylpentacene-5,14-diol (4). Halogen−metal exchange was performed according to the following procedure: *n*-BuLi (5.4 mL of a 1.6 M solution in hexane, 8.69 mmol) was added slowly by a syringe to a solution of 2,6-dimethylphenylbromide (1.36 g, 8.69 mmol) in THF (50 mL) at −78 °C. After complete addition of *n*-BuLi, the mixture was allowed to stir for 45 min at −78 °C and warmed slowly to room temperature. The resulting mixture was transferred slowly by cannula to a solution of pentacenequinone **1** (0.40 g, 0.87 mmol) in THF (200 mL) at 0 °C and then warmed to room temperature, stirred for 30 min then quenched by pouring into aqueous NH_4Cl (200 mL). The mixture was subsequently extracted with ethyl acetate, washed with brine, dried over $MgSO_4$, and concentrated in vacuo to yield crude red solid. The crude product was purified by column chromatography (silica gel, hexane/ethyl acetate = 16/1) and subsequent recrystallization from ethyl acetate/hexane to afford pure diol **4** (0.25 g, yield 43%). ^{1}H NMR ($CDCl_3$): δ 7.48−7.56 (m, 4H), 7.34−7.44 (m, 4H), 7.21−7.27 (m, 6H), 7.12−7.18 (m, 2H), 6.92−7.03 (m, 4H), 6.69−6.76 (dd, J = 12, 7.7 Hz, 4H), 6.17−6.21 (d, J = 7.8 Hz, 2H), 3.51 (s, 2H), 2.28 (s, 6H), 1.93 (s, 6H). ^{13}C NMR ($CDCl_3$): δ 146.4, 139.5, 138.1, 137.9, 137.7, 135.9, 132.8, 131.7, 131.4, 131.2, 130.5, 130.4, 128.2, 128.1, 127.9, 126.9, 126.7, 125.6, 79.8, 25.7, 24.3.

5,14-Bis(2,6-dimethylphenyl)-6,13-diphenylpentacene (DMPDPP) (5). To a solution of diol **4** (0.22 g, 0.32 mmol) in THF (30 mL) was added 3 mL of aqueous HI (55−57%) in a dark room. The dark mixture was allowed to react for 1 min, at which point a solid precipitated. After immediate filtering, the solid was washed with saturated aqueous $Na_2S_2O_5$ (3 × 100 mL), water (3 × 100 mL), and cold MeOH (3 × 100 mL), respectively. The combined solid was dissolved in diethyl ether, and the organic layer was washed with aqueous KOH (1 M), followed by brine. The organic layer was dried over $MgSO_4$ and concentrated in vacuo. Purification via double train sublimation gave pure product **5** as blue solid (54 mg, yield 26%). ^{1}H NMR ($CDCl_3$): δ 7.72 (s, 2H), 7.50−7.53 (dd, J = 6.6, 3.2 Hz, 2H), 7.02−7.16 (m, 8H), 6.94−6.99 (m, 10H), 6.77−6.80 (d, J = 7.5 Hz, 4H), 1.67 (s, 12H). ^{13}C NMR ($CDCl_3$): δ 140.9, 140.8, 137.4, 137.1, 135.1, 130.8, 130.1, 130.0, 129.7, 128.5, 127.4, 127.1, 127.0, 126.7, 126.5, 126.1, 125.7, 125.2, 124.9, 21.2. Anal. Calcd for $C_{50}H_{38}$: C, 94.00; H, 6.00. Found: C, 94.05; H, 5.98.

Optical Measurements. Spectroscopic grade solvents were degassed with nitrogen for 2 h prior to the optical measurements. Absorption spectra were recorded from 200 to 800 nm on a Hewlett-Packard 8453 spectrophotometer. Fluorescence spectra were obtained with an ISA Fluorolog-3 spectrofluorimeter equipped with a Xe lamp as an excitation source and were collected in the range 500−800 nm. The photo-oxidative stability of the pentacene derivatives was investigated by monitoring their optical spectra as a function of time after exposing samples to ambient air and light. The initial optical densities for pentacene derivatives in toluene solutions were ∼1.2. The quartz cells containing the toluene solutions were wrapped with metal foil and sealed to protect from ambient air and light. The solutions were exposed to ambient air and light, and their absorption spectra were recorded at specific time intervals.

Photoluminescence of Composite Films. Thin films of pentacene derivatives dispersed in the Alq_3 host were prepared by vacuum deposition and spectroscopically characterized. The films were prepared inside a vacuum chamber (pressure of 10^{-7} Torr), by co-deposition of the guest (pentacene derivatives) and host (Alq_3) molecules from separate resistive heating furnaces onto precleaned quartz substrates. The deposition rate of the guest and host molecules was monitored using a quartz crystal microbalance (nanogram sensitivity) and used to determine the composition and thickness of the films. The thickness of the composite films was ∼750 nm. Thin films were excited with 325 nm light from a HeCd laser source, and a GG 375 filter was placed in front of the collecting fiber to eliminate the scattered excitation light. PL spectra were obtained both in situ, in a vacuum, and ex situ, in a controlled atmosphere chamber filled with dry nitrogen using an ISA Spectrum One CCD (JY Spex). An integrating sphere was used to measure the absolute PL quantum yields (Φ_{PL}) of the composite films.[33] Light intensity scattered within the sphere was collected at the exit with a silicon photodiode, preceded by a Kodak-Wratten 2B filter (wavelength cutoff at 385 nm) and measured with an IL 1700 Research Radiometer.

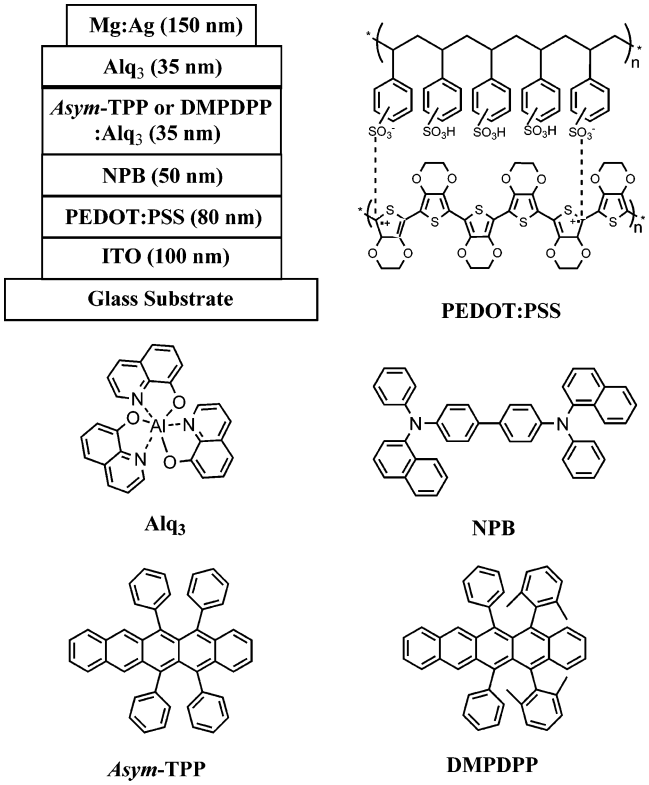

Figure 1. Materials and device structures for OLEDs.

Fabrication and Characterization of OLEDs. OLED devices were fabricated on glass substrates prepatterned with indium tin oxide (ITO) (sheet resistance of 30 Ω/□). The substrates were cleaned using a detergent and sonicated in deionized water, acetone, and 2-propanol, followed by treatment with oxygen plasma. The hole injection/buffer layer, poly(3,4-ethylenedioxythiophene):poly-(styrenesulfonate) (PEDOT:PSS, BAYTRON P VP CH 8000), was spin cast onto the treated ITO substrates and annealed to 130 °C for 5 min prior to mounting the substrates onto the wheel in the vacuum chamber. The devices were prepared by consecutive vapor deposition of the organic layers followed by vapor deposition of a Mg:Ag (∼13:1) alloy film. Figure 1 shows the chemical structures of the materials and the configuration of the devices used in this study. Here, 4,4′-bis[*N*-(1-naphthyl)-*N*-phenylamino]biphenyl (NPB) serves as the hole transport layer, and Alq_3 is used as both the electron transport layer and the host for the guest molecules (the pentacene derivatives). The composite films used as the active emitting layers were prepared by co-deposition of the guest

(33) Mattoussi, H.; Murata, H.; Merritt, C. D.; Iizumi, Y.; Kido, J.; Kafafi, Z. H. *J. Appl. Phys.* **1999**, *86*, 2642.

Scheme 1. Synthesis of Asymmetric Pentacene Derivatives *asym*-TPP and DMPDPP

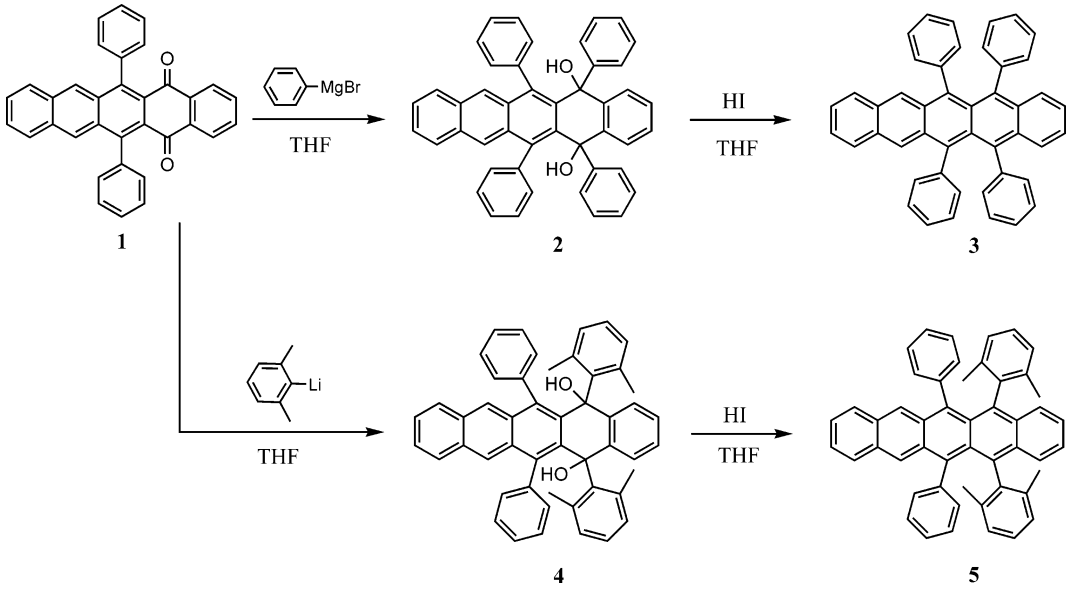

Scheme 2. Proposed Acid-Catalyzed Rearrangement of *asym*-TPP

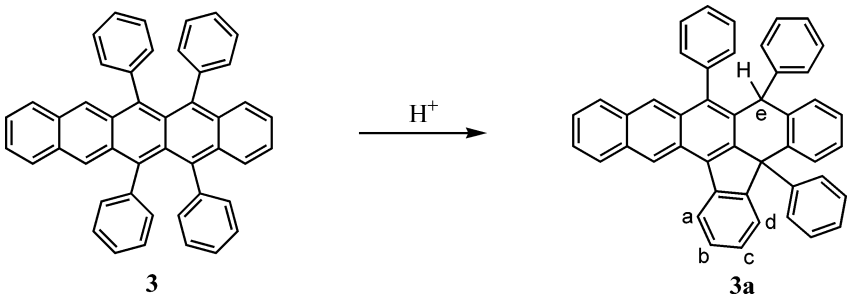

(pentacene derivatives) and host (Alq_3). The metal cathode (Mg:Ag alloy) was deposited through a shadow mask, affording four active areas (2×2 mm^2) per substrate. The device structure consisting of ITO (100 nm)/PEDOT:PSS (80 nm)/NPB (50 nm)/pentacene-doped Alq_3 (35 nm)/Alq_3 (35 nm)/Mg:Ag (150 nm) is shown in Figure 1.

Results and Discussion

Synthesis. Asymmetric pentacene derivatives, *asym*-TPP **3** and DMPDPP **5**, were prepared according to the synthetic route shown in Scheme 1. Pentacenediols **2** and **4** were synthesized via nucleophilic addition of phenylmagnesium bromide and 2,6-dimethylphenyllithium (prepared by halogen−metal exchange of 1-bromo-2,6-dimethylbenzene with *n*-butyllithium) to pentacenequinone **1**,[32] respectively, with reasonable chemical yields (30−43%). Initially, the reduction of diols with tin(II) chloride in aqueous acetic acid, often used in the conversion of 6,13-diarylpentacenediols to 6,13-diarylpentacene derivatives, was attempted but led to undesirable byproducts without the formation of the asymmetric pentacene derivatives. After several unsuccessful trials, the reductive aromatization of pentacenediols **2** and **4** using hydriodic acid and a brief reaction time (10−60 s) at room temperature yielded the corresponding asymmetric pentacene derivatives. Since polyaromatic hydrocarbon compounds (PAHs) such as anthracene and pentacene rapidly convert to their transannular peroxides upon exposure to air and light, the reactions were carried out in the dark.[31b,34]

Interestingly, the asymmetric pentacene derivatives formed in hydriodic acid quickly disappeared, yielding undesirable byproducts. The HI-catalyzed reductive aromatization of *peri* aryl-substituted pentacenediol **2** involves the formation of *asym*-TPP **3** followed by the spontaneous generation of an isomeric, ring-fused anthracene derivative **3a**,[35] which is derived from the acid-catalyzed rearrangement of *asym*-TPP **3** (Scheme 2). Similar rearrangement byproducts were isolated during the syntheses of 1,4,9,10-tetraphenylanthracene and rubrene.[36,37] DMPDPP **5** was much more stable than *asym*-TPP **3** toward the acid-catalyzed rearrangement because the sterically hindered xylyl groups effectively interfered with the cyclization of the adjacent cation.

Spectroscopic Characterization in Solutions. The absorption and PL spectra of the pentacene derivatives measured in toluene at room temperature are shown in Figure 2. These pentacene derivatives can be dissolved ($\sim 10^{-5}$ M) in common organic solvents such as chloroform and toluene

(34) Yamada, M.; Ikemoto, I.; Kuroda, H. *Bull. Chem. Soc. Jpn*. **1988**, *61*, 1057.
(35) Some characteristic ^{1}H NMR values of compound **3a** ($CDCl_3$, 300 MHz): δ 8.88 (d, $J = 8.3$ Hz, 1H), 8.47 (d, $J = 7.8$ Hz, 1H), 7.87 (m, 2H) [C(a), C(b), C(c), and C(d)], 5.41 (s, 1H) [C(e)]. MS (EI+): *m*/*z* 582 (M^+).
(36) Dickerman, S. C.; Souza, D.; Wolf, P. *J. Org. Chem.* **1965**, *30*, 1981.
(37) Hosokawa, T.; Nakano, H.; Takami, K.; Kobiro, K.; Shiga, A. *Tetrahedron Lett.* **2003**, *44*, 1175.

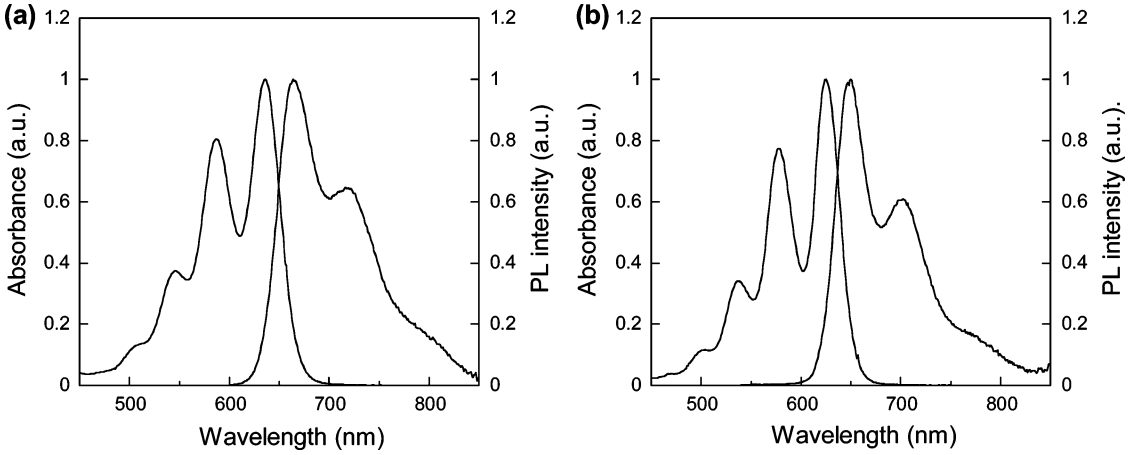

Figure 2. Absorption and PL spectra of (a) *asym*-TPP and (b) DMPDPP in toluene.

but in general show slightly lower solubility compared to 6,13-diphenylpentacene (DPP). The absorption and emission maxima of *asym*-TPP and DMPDPP are centered at 636 and 664, and 625 and 650 nm, respectively. Both absorption and emission maxima of bis(2,6-dimethylphenyl)-substituted pentacene (DMPDPP) are slightly blue-shifted relative to those of the asymmetrically tetraphenyl-substituted pentacene (*asym*-TPP). This blue shift suggests that the steric hindrance caused by the *ortho* methyl groups of the 2,6-dimethylphenyl moiety on DMPDPP may lead to further rotation (out-of-plane) of the xylyl groups and interrupt the extended π-conjugation between the pentacene unit and the aryl substituents. This behavior is similar to and consistent with the observed blue shift in the absorption and fluorescence spectra of 6,13-bis(2,6-dimethylphenyl)pentacene (DMPP) relative to those of 6,13-diphenylpentacene (DPP).[14] Both toluene solutions of *asym*-TPP and DMPDPP show relatively large Stoke shifts (25−28 nm) compared to those of the 6,-13-diaryl-substituted analogues (3−10 nm), suggesting that the molecule undergoes considerable molecular rearrangement upon photoexcitation.

Photo-Oxidation Stability in Solutions. The photo-oxidative stability of 5,7,12,14-tetraphenylpentacene (*sym*-TPP), *asym*-TPP, and DMPDPP was measured using optical (UV−vis) spectroscopy. Solutions of all pentacene derivatives (initial OD ~1.2) were exposed to ambient light and air. Figure 3 shows the depletion of their absorbance maxima (617, 625, and 636 nm for *sym*-TPP, *asym*-TPP, and DMPDPP, respectively) as a function of time. The asymmetrically aryl-substituted pentacenes (*asym*-TPP and DMPDPP) containing the aryl groups at the 6- and 13-carbon positions thus protecting the most reactive sites are much more stable than the *sym*-TPP, where photo-oxidation at the 6,13 position can readily occur. The rate constants for the photo-oxidation processes for *sym*-TPP, *asym*-TPP, and DMPDPP (fitted to an exponential decay) were calculated to be 6.25×10^{-3}, 5.06×10^{-4}, and 3.90×10^{-4} s^{-1}, respectively. The asymmetric pentacene derivatives, *asym*-TPP and DMPDPP, exhibited slightly more than an order of magnitude smaller photo-oxidation rate constants compared to the *sym*-TPP. This result demonstrates that the *sym*-TPP with the unprotected site, the bare reactive central carbon, is the most vulnerable to photo-oxidation. Upon

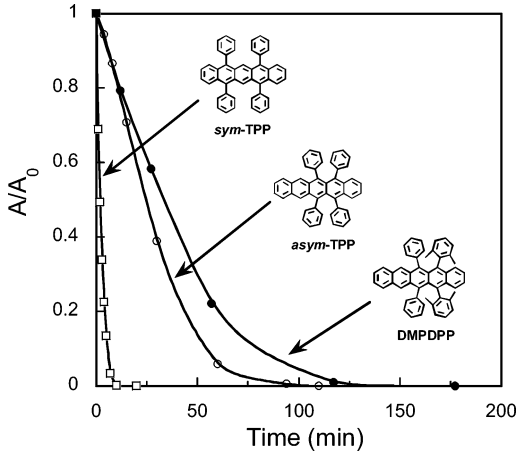

Figure 3. Absorption maxima (normalized to initial value) of toluene solutions of *sym*-TPP (□), *asym*-TPP (○), and DMPDPP (●) upon exposure to air as a function of time.

exposure to oxygen, it undergoes rapid conversion to *endo*-peroxide.[31] DMPDPP proved to be the most photo-oxidatively stable of the three compounds. Since the aryl substituents are twisted out of the plane of the adjacent polyacene unit (large torsion angle),[38] the methyl groups of DMPDPP lying above and below the reactive central carbons impede the approach of oxygen leading to its enhanced photo-oxidative stability.[14]

Electrochemical Study. Cyclic voltammetry (CV) was applied to measure the oxidation and reduction potentials of the pentacenes, determine the stability of their oxidized and reduced forms, and assess the positions of their molecular orbital energy levels as well as estimate their solid-state ionization potential, electron affinity, and HOMO (the highest occupied molecular orbital)−LUMO (the lowest unoccupied molecular orbital) gaps. The electrochemical properties of *asym*-TPP and DMPDPP were investigated using a glassy carbon electrode versus $Ag/AgNO_3$ in 1,2-dichlorobenzene/tetrabutylammonium perchlorate (0.1 M). Representative cyclic voltammograms of *asym*-TPP and DMPDPP are shown in Figure 4 and compared with that of DPP (as a reference compound). The electronic properties of DPP in the solid have been characterized using a combination of

(38) Becker, H.-D.; Langer, V.; Sieler, J.; Becker, H.-C. *J. Org. Chem.* **1992**, *57*, 1883.

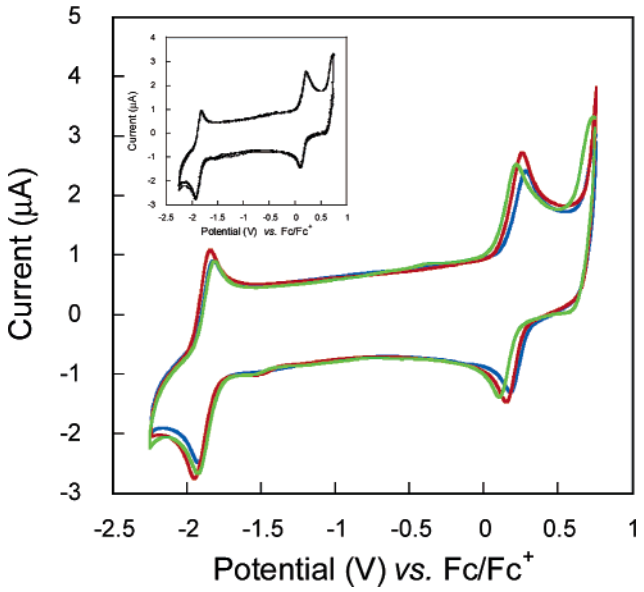

Figure 4. Cyclic voltammograms of *asym*-TPP (green line), DMPDPP (red line), and DPP (blue line) in 1,2-dichlorobenzene containing $Bu_4N^+ClO_4^-$ (0.1 M) with a scan rate of 100 mV/s. The inset shows the multiscans of *asym*-TPP (4 cycles).

ultravilolet photoelectron spectroscopy (UPS) and UV−vis absorption spectroscopy.[12] As shown in Figure 4, both one-electron oxidation and reduction processes for each of the pentacenes are reversible, demonstrating excellent electrochemical stability of their cations and anions. For tetraphenyl-substituted *asym*-TPP, the measured half-wave oxidation potential ($E_{1/2}$) is 0.16 V which is smaller than that of DPP (0.24 V), whereas the half-wave reduction potential is identical to that of DPP (−1.87 V). This result suggests that the additional phenyl groups perturb the HOMO energy level without affecting the LUMO energy level. To gain further insights (change) into the nature of electrochemical stability of asymmetrically tetra(aryl)-substituted pentacenes, multiscans (4 cycles) of the consecutive oxidation and reduction processes for *asym*-TPP were performed (inset in Figure 4). No change in the CV curve of *asym*-TPP was observed in the range −2.25 to +0.75 V. This result indicates that the asymmetrically substituted pentacenes are electrochemically stable which is very important for the long-term operation of many devices incorporating them such as OFETs, OPVs, and OLEDs.

Replacing the phenyl group with 2,6-dimethylphenyl moiety at the 5 and 14 positions on the pentacene backbone led to an increase in the oxidation potential of DMPDPP (0.21 V) relative to that of *asym*-TPP. On the other hand, the reduction potential of DMPDPP (−1.89 V) is very similar to that of *asym*-TPP. As a result, the estimated HOMO−LUMO band gap of DMPDPP (2.10 eV) is slightly larger than that of *asym*-TPP (2.03 eV), consistent with the blue shift observed in their optical spectra. This result confirms that the steric hindrance introduced by the *ortho* dimethylphenyl group on DMPDPP disrupts the extended π-conjugation between the pentacene backbone and the aryl substituents. The estimated band gaps of the aryl-substituted pentacenes (2.0−2.1 eV) are also consistent with the measured optical band gaps (1.9−2.0 eV).

Table 1. Electrochemical Properties of Aryl-Substituted Pentacenes

compd	$E_{1/2}^{ox}$ [a] (V)	$E_{1/2}^{red}$ [a] (V)	E_{HOMO} [b] (eV)	E_{LUMO} [b] (eV)	E_g (eV)
asym-TPP	0.16	−1.87	−4.96	−2.93	2.03
DMPDPP	0.21	−1.89	−5.01	−2.91	2.10
DPP	0.24	−1.87	−5.04 (−5.2)[c]	−2.93	2.11
Alq_3	0.73[d]	−2.30[d]	−5.53	−2.50	3.03

[a] Determined from cyclic voltammetry in 1,2-dichlorobenzene using Ag/$AgNO_3$ (0.01 M) as a reference electrode at a scan rate of 100 mV/s. [b] HOMO and LUMO levels were determined using the following equations: E_{HOMO} (eV) = $-e(E_{1/2}^{ox} + 4.8)$, E_{LUMO} (eV) = $-e(E_{1/2}^{red} + 4.8)$. [c] Determined from UPS study. [d] Reference 40.

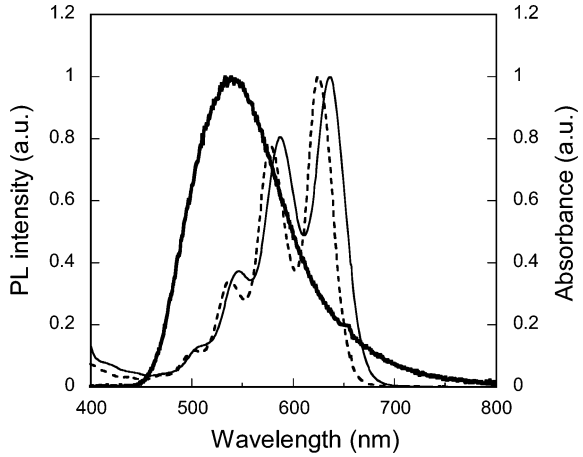

Figure 5. PL spectrum of a film of Alq_3 (bold line) and absorbance spectra of *asym*-TPP (thin line) and DMPDPP (dashed line) in toluene.

The HOMO and LUMO energy levels of the pentacene derivatives were estimated according to the empirical formulas $E_{HOMO} = -e(E^{ox} + 4.8)$ (eV) and $E_{LUMO} = -e(E^{red} + 4.8)$ (eV) based on an ionization energy (−4.8 eV below the vacuum level) for ferrocene/ferrocenium (Fc/Fc^+).[39] They are summarized in Table 1. As mentioned above, the LUMO energy levels of the three pentacenes estimated from the electrochemical data are almost identical (−2.9 eV), and are similar to that of DPP (derived from the combined UPS data and the measured optical band gap). In addition, the HOMO and LUMO energy levels of all three pentacene derivatives lie within those of the Alq_3 host ($E_{HOMO} = -5.53$ eV and $E_{LUMO} = -2.50$ eV).[40]

Spectroscopic Characterization of the Solid Films. Alq_3 was chosen as the host material for the pentacene derivatives. The emission spectrum of a film of neat Alq_3 and the absorption spectra of solutions of *asym*-TPP and DMPDPP are given in Figure 5. The emission spectrum of Alq_3 overlaps well with the absorption spectra of the pentacene derivatives, which is critical for efficient energy transfer from the host to the guest molecules.[12] A 10 nm blue shift in the absorption of DMPDPP relative to that of *asym*-TPP leads to a slightly better spectral overlap with the emission of Alq_3.

Figure 6 shows the PL spectra of composite films of the pentacene derivatives dispersed in Alq_3 at various guest concentrations. The PL spectra are dominated by the red emission from the guest molecules signaling efficient Förster energy transfer from the host (Alq_3) to guest molecules

(39) Lee, S. H.; Jang, B.-B.; Tsutsui, T. *Macromolecules* **2002**, *35*, 1356.
(40) Armstrong, N. R. et al. *J. Am. Chem. Soc*. **1998**, *120*, 9646.

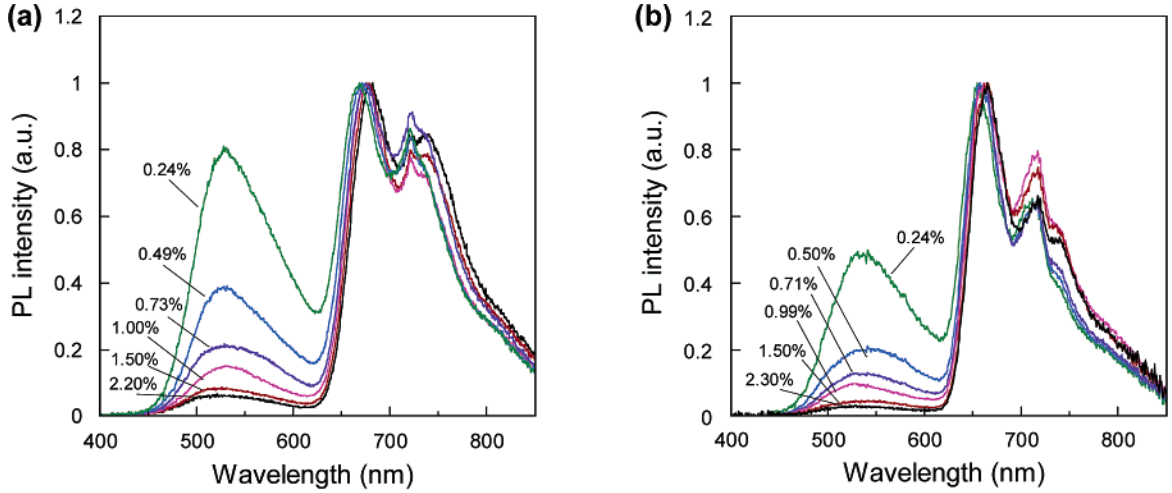

Figure 6. PL spectra of composite films of (a) *asym*-TPP and (b) DMPDPP dispersed in Alq_3 as a function of guest molecule concentrations, expressed in mol %.

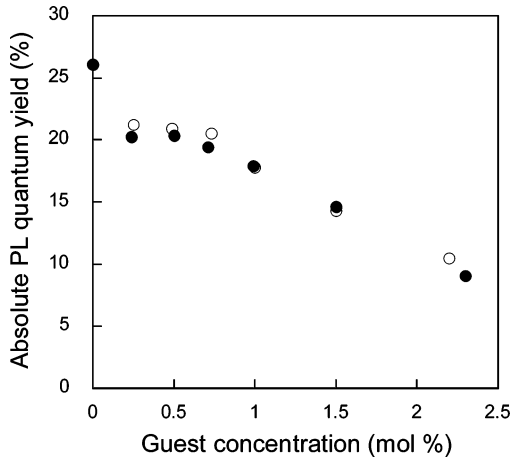

Figure 7. Absolute PL quantum yields (Φ_{PL}) of films of *asym*-TPP (○) and DMPDPP (●) dispersed in Alq_3 as a function of guest molecule concentrations.

(*asym*-TPP and DMPDPP).[41] The *asym*-TPP and DMPDPP have emission maxima centered at 679 and 663 nm which are red-shifted (15 and 13 nm, respectively) relative to their solution values. The differences are likely due to the change in the dielectric constants of the surrounding solid. The contribution of Alq_3 emission around 550 nm decreases as the concentration of the pentacene derivatives increases from 0.24 to 2.30 mol %, leading to a purer red emission. A smaller contribution of the Alq_3 emission was observed for DMPDPP relative to that of *asym*-TPP at similar concentrations, which demonstrates more efficient Förster energy transfer and is consistent with the better spectral overlap between the absorption of DMPDPP and the emission of Alq_3.

Figure 7 shows the absolute PL quantum yields (Φ_{PL}) of films of the pentacene derivatives dispersed in Alq_3 as a function of guest molecule concentrations. The maximum absolute PL quantum yields of *asym*-TPP and DMPDPP are measured to be 21% and 20%, respectively, at low concentrations (0.25−0.50 mol %), and are somewhat lower than those of their DPP analogues (Φ_{PL} = 30−32%). Figure 7 shows that the PL quantum yield gradually drops off as the guest concentration increases, probably due to self-quenching caused by aggregation.

Electroluminescence Spectra. In Figure 8, the electroluminescence spectra of OLEDs based on the pentacene derivatives (*asym*-TPP and DMPDPP) dispersed in Alq_3 are depicted as a function of guest molecule concentrations (0.24−2.40 mol %). The EL spectra of *asym*-TPP are characterized by a strong red emission peak centered at 679 nm with a smaller one at 743 nm. The contribution from Alq_3 in the EL spectra gradually decreases as the concentration of the guest molecule increases. The strong emission observed for DMPDPP is centered at 663 nm with smaller peaks at longer wavelengths (725−750 nm). The EL spectra are all similar to the PL spectra of the corresponding composite films, suggesting that light emission originates from the same singlet excited states. The CIE (Commission Internationale de l'Eclairage) chromaticity coordinates for the OLED based on *asym*-TPP:Alq_3 emitting layer were estimated to be (x = 0.60, y = 0.38) at high guest concentration (2.40 mol %) (inset in Figure 8a). Using an OLED based on a DMPDPP:Alq_3 emitting layer, a saturated red emission was achieved with CIE chromaticity coordinates (x = 0.67, y = 0.32), which is very close to the National Television Standards Committee (NTSC) red specification (x = 0.67, y = 0.33) (inset in Figure 8b).

Further comparison between the EL and PL spectra shows a smaller contribution from Alq_3 in the EL spectra at a given guest concentration (∼0.50 mol %) (Figure 9). This reduction in the Alq_3 contribution observed in the EL spectra relative to the PL spectra is observed for both guest molecules ((a) *asym*-TPP and (b) DMPDPP), similar to what was previously reported in OLEDs based on DPP derivatives.[12,14] The smaller contribution from the host in the EL spectra suggests that another EL mechanism is taking place in addition to Förster energy transfer from the host to guest, which is the only operative PL mechanism. Direct carrier (electron−hole) recombination on the guest molecules is proposed and was previously reported as the dominant EL mechanism for OLEDs based on DPP derivatives.[12,42,43] The HOMO−LUMO gap of the guest molecules needs to lie within the

(41) Palilis, L. C.; Melinger, J. S.; Wolak, M. A.; Kafafi, Z. H. *J. Phys. Chem. B* **2005**, *109*, 5456.

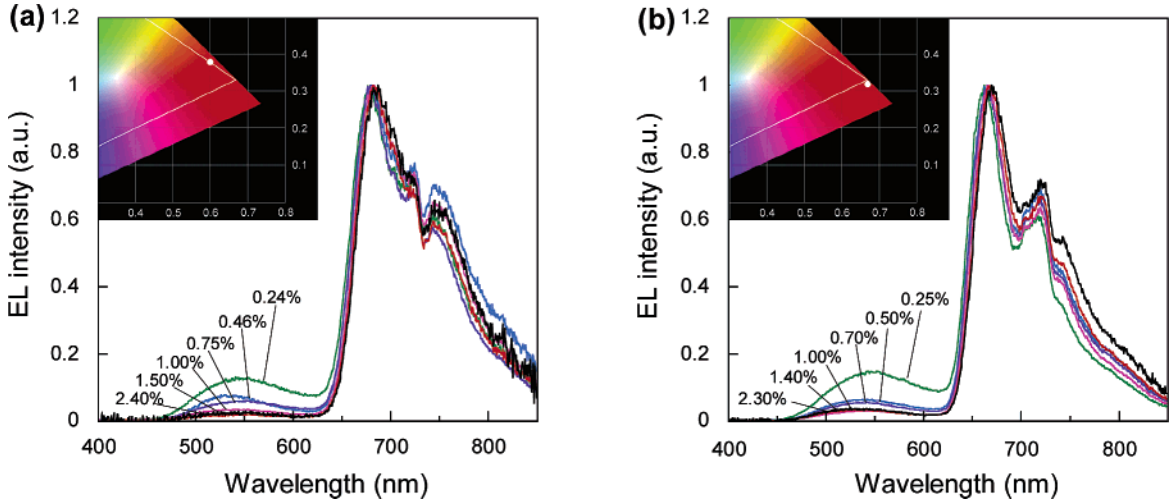

Figure 8. EL spectra of OLEDs based on the active emitting layers (a) *asym*-TPP:Alq_3 and (b) DMPDPP:Alq_3 at various guest molecule concentrations, expressed in mol %. The insets show CIE chromaticity coordinates for OLEDs based on *asym*-TPP (2.40 mol %) and DMPDPP (2.30 mol %) dispersed in Alq_3.

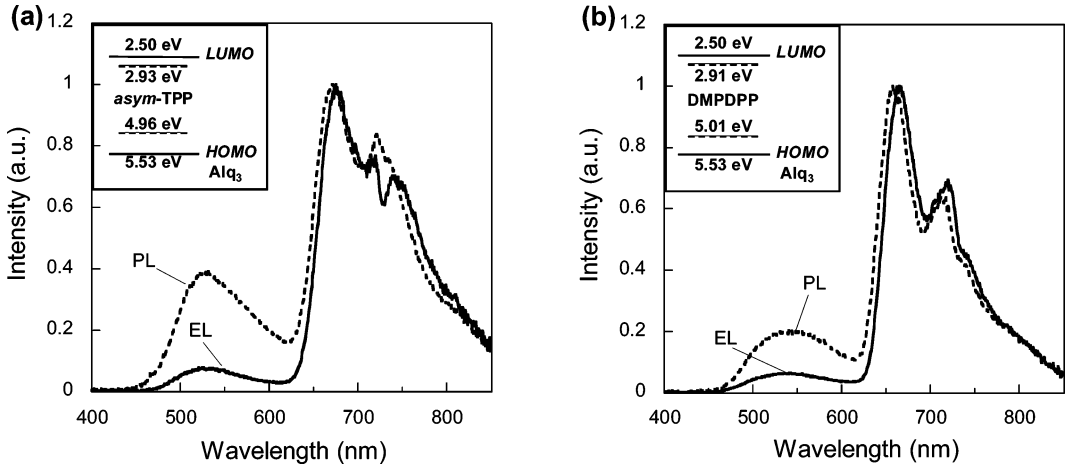

Figure 9. PL (dashed line) and EL (solid line) spectra of the active emitting layers containing 0.50 mol % pentacenes ((a) *asym*-TPP and (b) DMPDPP) dispersed in Alq_3. The insets show the energy-level diagrams for neat organic films of the guest and host molecules derived from the CV data.

gap of the host matrix in order for this EL mechanism to be operative. In this case (see insets in Figure 9), the pentacenes may act as a hole or electron trap, and hopping of the carrier with the reverse polarity leads to direct electron−hole recombination on the guest molecules.

***J*−*V* Characteristics of OLEDs.** The current density (*J*) versus voltage (*V*) characteristics for the OLEDs based on *asym*-TPP dispersed in Alq_3 are shown in Figure 10 at several guest molecule concentrations. The results are consistent with the proposed EL mechanism where the guest molecules act as charge carrier traps. This is clearly seen in the voltage dependence on the guest molecule *asym*-TPP concentrations where it increases as a function of the pentacene concentrations. For example, a current density of 100 A/m^2 is achieved at 9 V for the device based on the *asym*-TPP (0.24 mol %). At high guest concentration (2.40 mol %), a dramatic increase in the driving voltage (17.5 V) is required in order to attain the same current density (100 A/m^2).

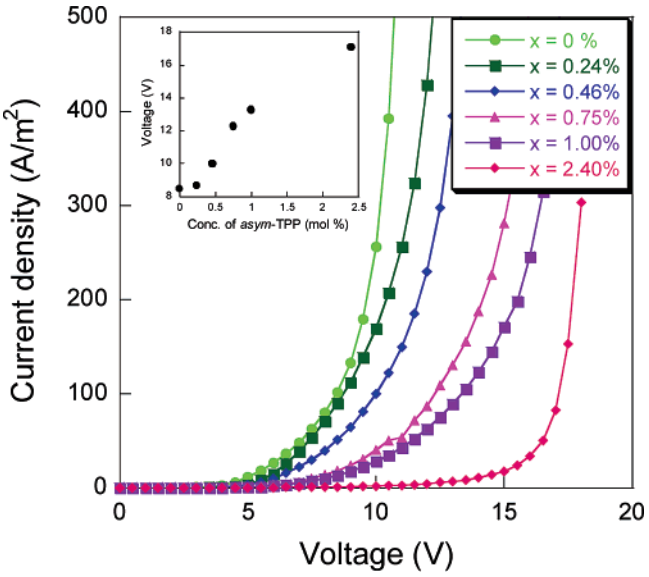

Figure 10. *J*−*V* characteristics for OLEDs based on *asym*-TPP dispersed in Alq_3 as a function of guest molecule concentration, expressed in mol %. The inset shows the voltage as a function of guest molecule concentration at a current density of 100 A/m^2.

(42) Kafafi, Z. H.; Murata, H.; Picciolo, L. C.; Mattoussi, H.; Merritt, C. D.; Iizumi, Y.; Kido, J. *Pure Appl. Chem.* **1999**, *71*, 2085.
(43) Murata, H.; Merritt C. D.; Kafafi, Z. H. *IEEE J. Sel. Top. Quantum Electron.* **1998**, *4*, 119.

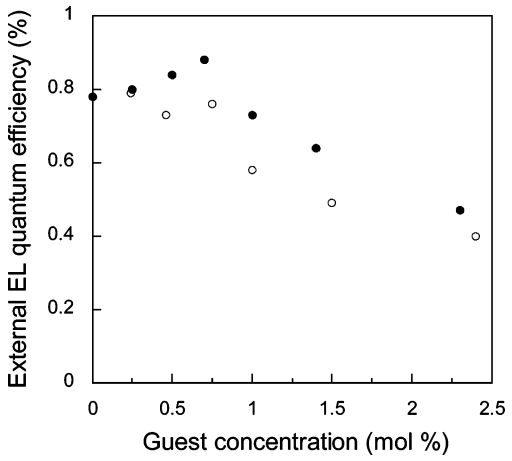

Figure 11. External EL quantum efficiency as a function of guest molecule concentration at a current density of 100 A/m^2: *asym*-TPP (○) and DMPDPP (●).

External EL Quantum Efficiency. The external EL quantum efficiency (η_{EL}) for an OLED device may be simply expressed as[44]

$$\eta_{EL} = \alpha\gamma\eta_r\phi_{PL}$$

where α is the light output coupling factor (which is a function of the refractive index (n) of the emissive medium $\alpha = 1/2n^2$), γ is the probability of carrier recombination, η_r is the singlet to triplet branching ratio governed by spin statistics, and ϕ_{PL} is the absolute PL quantum yield of the emissive layer. Using the measured ϕ_{PL} ~20% for either pentacene and assuming $\alpha = 0.20$ ($n = 1.7$ for Alq_3),[45] $\gamma = 1.0$, and $\eta_r = 0.25$, a theoretical limit of ~1% is estimated for the OLED devices based on *asym*-TPP and DMPDPP.

As shown in Figure 11, the maximum η_{EL} for the device based on DMPDPP is measured to be 0.9% (0.70 mol %), very close to the theoretical limit of 1% (based on fluorescence). The external EL quantum efficiencies (η_{EL}) of the OLED measured at a current density of 100 A/m^2 (Figure 11) show a similar concentration dependence to those of the PL quantum yields but fall at a slower rate with increasing concentration, consistent with the proposed additional EL mechanism, i.e., direct electron−hole recombination on the pentacene guest molecules.

Conclusion

In summary, we have presented a facile route to synthesize novel asymmetrically aryl-substituted pentacene derivatives and successfully incorporated them as red emitters in OLEDs. Reductive aromatization of *peri* aryl-substituted pentacenediols to the corresponding pentacenes was optimized using hydriodic acid with short reaction time at room temperature. These pentacene derivatives show reasonable photochemical and electrochemical stability. We demonstrated that OLEDs based on these fluorescent pentacenes (*asym*-TPP and DMPDPP) exhibit an external EL quantum efficiency close to the estimated theoretical limit (1%) based on their measured PL quantum yields.

Acknowledgment. This work was financially supported by the Office of Naval Research. Special thanks to Dr. Woohong Kim for helping to prepare the PEDOT:PSS-ITO treated substrates and to Dr. Mason A. Wolak for his insightful comments.

Supporting Information Available: Complete ref 40 including full list of authors. This material is available free of charge via the Internet at http://pubs.acs.org.

CM052069H

(44) (a) Tsutsui, T. *MRS Bull.* **1997**, *22*, 39. (b) Picciolo, L. C.; Murata, H.; Kafafi, Z. H. *Proc. SPIE-Int. Soc. Opt. Eng.* **2001**, *4105*, 474.
(45) Greenham, N. C.; Friend, R. H.; Bradley, D. D. C. *Adv. Mater.* **1994**, *6*, 491.